

[¹⁸F]DPA-714 PET Imaging of AMD3100 Treatment in a Mouse Model of Stroke

Yu Wang,^{†,‡} Xuyi Yue,[‡] Dale O. Kiesewetter,[‡] Zhe Wang,[‡] Jie Lu,[‡] Gang Niu,^{*,‡} Gaojun Teng,^{*,†} and Xiaoyuan Chen^{*,‡}

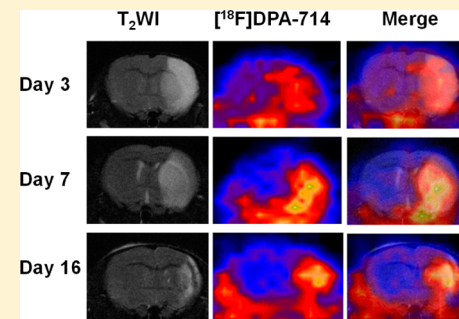
[†]Jiangsu Key Laboratory of Molecular Imaging and Functional Imaging, Department of Radiology, Zhongda Hospital, Medical School of Southeast University, Nanjing 210009, China

[‡]Laboratory of Molecular Imaging and Nanomedicine, National Institute of Biomedical Imaging and Bioengineering, National Institutes of Health, Bethesda, Maryland 20892, United States

Supporting Information

ABSTRACT: Chemokine receptor 4 and stromal-cell-derived factor 1 have been found to be related to the initiation of neuroinflammation in ischemic brain. Herein, we aimed to monitor the changes of neuroinflammation after AMD3100 treatment using a translocator protein (TSPO) specific PET tracer in a mouse model of stroke. The transient MCAO model was established with Balb/C mice. The success of the model was confirmed by magnetic resonance imaging and FDG PET. The treatment started the same day after surgery via daily intraperitoneal injection of 1 mg of AMD3100/kg for three consecutive days. [¹⁸F]DPA-714 was used as the TSPO imaging tracer. *In vivo* PET was performed at different time points after surgery in both control and treated mice. *Ex vivo* histological and immunofluorescence staining of brain slices was performed to confirm the lesion site and inflammatory cell activation. The TSPO level was also evaluated using Western blotting. Longitudinal PET scans revealed that the level of [¹⁸F]DPA-714 uptake was significantly increased in the ischemic brain area with a peak accumulation at around day 10 after surgery, and the level of uptake remained high until day 16. The *in vivo* PET data were consistent with those from *ex vivo* immunofluorescence staining. After AMD3100 treatment, the signal intensity was significantly decreased compared with that of normal saline-treated control group. In conclusion, TSPO-targeted PET imaging using [¹⁸F]DPA-714 can be used to monitor inflammatory response after stroke and provide a useful method for evaluating the efficacy of anti-inflammation treatment.

KEYWORDS: stroke, AMD3100, translocator protein (TSPO), DPA-714, PET



INTRODUCTION

Ischemic stroke is a leading cause of mortality and morbidity in the world. Each year, ~100000 people experience a new or recurrent stroke.¹ Although the pathologic mechanisms of the life-threatening disease are still not clear, it has been well accepted that neuroinflammation is a key component of the pathogenic cascade after ischemic damage in the brain.² Although the activated glia cells can encapsulate the infarct or enhance neuronal plasticity,^{3,4} lymphocyte infiltration is detrimental because of the hampering of axonal growth.⁵ Indeed, the inflammatory response during the brain remodeling period after injury is considered to be a negative factor for the regenerative process. The long-lasting neuroinflammation induced by Wallerian degeneration in local infarction, the remote area, and the connecting fibers could further lead to the loss of brain function.⁴ Therefore, anti-inflammatory strategies have been adopted to improve stroke outcome.^{6,7}

Chemokine receptor 4 (CXCR4) and stromal-cell-derived factor 1 (SDF-1) are constitutively expressed by microglia and astrocytes in both developing and mature central neural systems (CNSs). This pathway has a recognized role in brain

inflammation and neuromodulation.⁸ After experimental stroke, the level of expression of SDF-1 is elevated for several days and closely associated with the infiltration of CXCR4-expressing cells.⁹ When ischemic injury happens, the level of expression of SDF-1 is elevated in the peri-infarct and infarct region.¹⁰ This phenomenon appears to be related to the initiation of a cascade of events leading to neuroinflammation, such as local microglia activation and peripheral monocyte and leukocyte migration to the central neural system (CNS) against a SDF-1 concentration gradient.^{11–15} In view of this, the SDF-1 pathway has been proposed to be an attractive pharmacological target for modulating the recruitment of immune cells into the ischemic territory and improving functional recovery after stroke. Indeed, Ruscher et al.¹⁶ found that inhibition of the SDF-1/CXCR4 pathway with AMD3100, a specific antagonist of CXCR4, suppresses the invasion of the ischemic territory by peripheral

Received: March 28, 2014

Revised: August 21, 2014

Accepted: August 26, 2014

Published: August 26, 2014

immune cells, which promotes the recovery of function. In another study, AMD3100 significantly inhibited the inflammatory response and reduced the extent of blood–brain barrier disruption after MCAO by attenuating ischemia-induced acute inflammation by suppressing leukocyte migration and infiltration.⁷

The acute inflammatory responses consist of local microglia activation, peripheral immune cell migration, and proinflammatory cytokine and chemokine secretion, while chronic inflammation in CNS is mainly characterized by angiogenesis, glial scar formation, and nutritious cytokine secretion.² Therefore, a better understanding of these complicated processes will be the starting point for developing curative treatments. Recently, PET imaging of translocator protein (TSPO) has been investigated as a noninvasive strategy for evaluating neuroinflammation.^{17–21} TSPO is an 18 kDa protein that is localized at the outer mitochondrial membrane of different cell types.^{22,23} It is expressed at low levels in healthy brain but is robustly upregulated in response to injury and inflammation. In cerebral ischemia, the level of expression of TSPO is increased in activated microglia as well as in macrophages and neutrophils entering the brain from the peripheral blood within the first days after the insult.²⁴ Among the various radiolabeled TSPO ligands, [¹⁸F]DPA-714 shows a comparatively high specificity and binding potential in different disease models such as cerebral ischemia, herpes encephalitis, and chemically induced acute neuroinflammation.^{25–27} Studies of [¹⁸F]DPA-714 in healthy volunteers further confirm its potential use in the diagnosis of CNS diseases and perhaps therapeutic efficacy monitoring.²⁸

In this study, we developed a mouse MCAO model and treated the mice that had suffered strokes with AMD3100 to alleviate injury-induced neuroinflammation. The inflammatory response was evaluated with [¹⁸F]DPA-714 PET imaging longitudinally. We expected to identify the causal relationship between AMD3100 treatment and the change in TSPO expression level after stroke and investigate its potential anti-inflammation property. The long-term goal of this study is to apply TSPO PET imaging for optimizing the anti-inflammatory intervention of ischemic brain injuries.

MATERIALS AND METHODS

General. All reagents were of analytical grade and were obtained from commercial sources. [¹⁸F]F[−] radionuclide was obtained from the National Institutes of Health Clinical Center's cyclotron facility by proton irradiation of ¹⁸O-enriched water. [¹⁸F]FDG was purchased from the Nuclear Pharmacy of Cardinal Health and diluted, as necessary, with sterile saline. Automated synthesis of [¹⁸F]DPA-714 was conducted using a slightly modified TRACERLab FX-FN module (GE Medical Systems).^{29,30}

Middle-Cerebral-Artery Occlusion (MCAO) Model. All animal studies were approved by the Institutional Animal Care and Use Committee of the Clinical Center of the National Institutes of Health. All the experiments were conducted in accordance with the principles and procedures outlined in the Guide for the Care and Use of Laboratory Animals.³¹

Transient MCAO was induced in male Balb/c mice weighing 25–30 g as previously reported with modifications.³² Briefly, mice were anesthetized in a ventilated chamber with isoflurane (3.5% for induction and 2% for maintenance) and then placed under a stereomicroscope in a supine position. A warming pad was used to keep the body temperature at 37 °C during the

surgery. A midline skin incision was made at the neck region followed by careful exposure of the external, internal, and common carotid arteries (ECA, ICA, and CCA, respectively). One silicone-coated 6-0 MCAO suture (602356PK10, Doccil MCAO suture) was gently advanced into the ICA to block the blood flow of the middle cerebral artery for 60 min. After that, the suture was moved out for reperfusion of the ischemic brain area. Sham-treated controls underwent artery exposure without suture insertion.

For treatment, AMD3100 (Santa Cruz Biotechnology) was injected intraperitoneally for three consecutive days with the first injection performed immediately after the surgery with a dose of 1 mg/kg/day.⁷ The mice in the control group were injected with the same volume of saline.

Magnetic Resonance Imaging (MRI). All MRI was performed on a high-field micro-MR scanner (7.0 T, Bruker, Pharmascan) with a body coil. Mice were anesthetized with isoflurane (3.5% for induction and 1.5% for maintenance) and kept warm with a circulating water pad that covered the whole coil. Magnetic T₂-weighted images were obtained by a RARE sequence with a respiratory-gating technology. The parameters were as follows: TR, 3000 ms; effective TE, 70 ms; NEX, 4; matrix size, 256 × 256; FOV, 4 cm × 4 cm; and slice thickness, 1 mm.

Positron Emission Tomography and Data Analysis. For the longitudinal study, [¹⁸F]FDG PET was performed 1, 3, 10, and 16 days after MCAO ($n = 3–6$), while static [¹⁸F]DPA-714 imaging was performed on days 0, 1, 3, 7, 10, and 16 with another group of MCAO mice ($n = 4–6$). Another eight mice were used as sham controls for [¹⁸F]FDG and [¹⁸F]DPA-714 imaging. For the acquisition of static images, a single dose of 3.7 MBq (100 μCi) of [¹⁸F]FDG or [¹⁸F]DPA-714 was injected into animals intravenously under isoflurane anesthesia. One hour after the tracer had been injected, a 15 min static PET scan was performed with a heating pad to keep anesthetized animals warm. For the [¹⁸F]DPA-714 displacement study, a 1 h dynamic acquisition was performed on mice 6 days after MCAO with ($n = 3$) or without ($n = 3$) 5 mg of unlabeled PK11195/kg administered via an intravenous catheter 30 min after tracer injection. For the treatment study, static [¹⁸F]DPA-714 imaging with the same parameters that were used in the longitudinal study was performed on 3 and 7 days after MCAO surgery in both the AMD3100-treated group ($n = 10$) and the saline-treated control group ($n = 10$).

All PET images were acquired with an Inveon small animal PET scanner (Siemens Preclinical Solutions). All the images were reconstructed using a two-dimensional ordered-subset expectation maximum algorithm (2D OSEM). Three-dimensional ellipsoidal regions of interest (ROIs) were manually defined on the ischemic region in the ipsilateral hemisphere under the guidance of T₂-weighted MR images of each mouse obtained at the same time points of PET imaging. Another ROI with the same shape was drawn on the corresponding region in the contralateral brain sphere as normal background signals. The mean pixel value of each ROI was measured with Inveon Research Workshop software (Siemens Preclinical Solution). The value was then converted to the concentration of radioactivity in units of megabecquerels per milliliter. The image-derived tissue uptake, presented as percent injected dose per gram (%ID/g), was obtained with tissue radioactivity divided by injected dose assuming a tissue density of 1 g/mL.³³

Immunofluorescence Staining. Brain cryosections with a thickness of 8 μm were obtained using an Ultrapro 5000

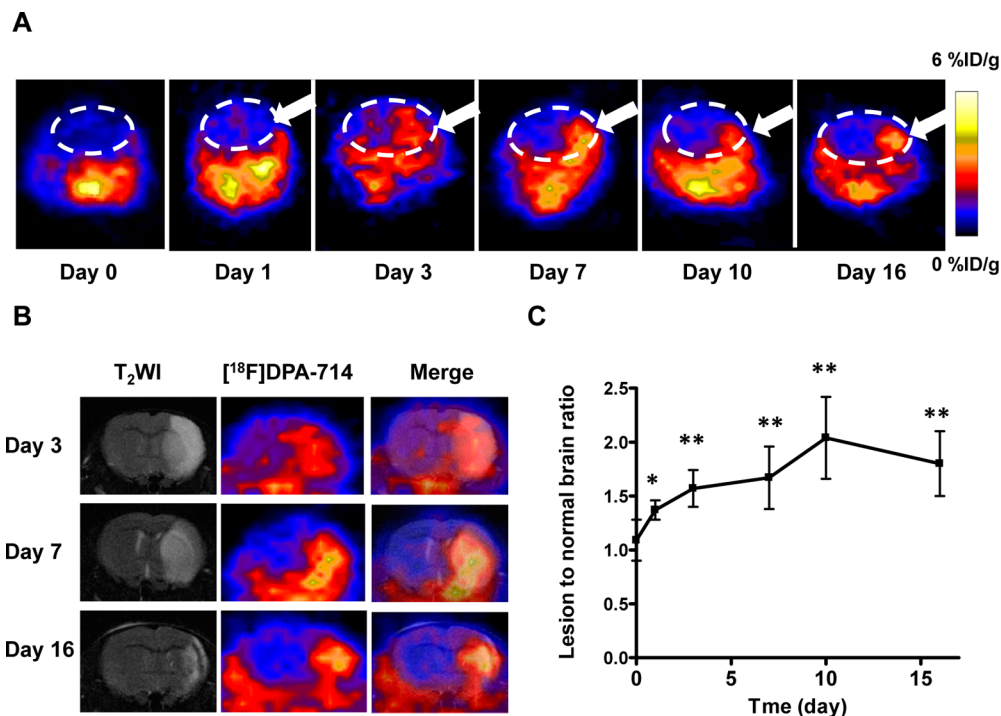


Figure 1. $[^{18}\text{F}]$ DPA-714 PET imaging of TSPO expression. (A) Representative coronal PET images of $[^{18}\text{F}]$ DPA-714 at the lesion area after surgery. The white dashed line shows the brain area and the white arrow the damaged region. (B) Representative coronal T_2 -weighted MRI, $[^{18}\text{F}]$ DPA-714 PET, and coregistered images at different time points after MCAO surgery. (C) Quantification of $[^{18}\text{F}]$ DPA-714 uptake over time after MCAO surgery. The uptake ratio increased significantly from day 1 to day 16 compared with the baseline level before surgery (* $p < 0.05$; ** $p < 0.01$).

cryostat (Vibratome). Both brain sections and cells were fixed with Z-fix solution for 15 min and then blocked with phosphate-buffered saline (PBS) containing 1% bovine serum albumin (BSA) for 0.5 h. Slices were incubated with primary antibodies at 4 °C overnight and with secondary antibodies in a dark area for 60 min at room temperature. After each step, slices were washed gently three times with PBS containing 0.05% Tween 20 (PBST) for 5 min. For different staining targets, the primary antibodies and concentrations are as follows: rat anti-mouse TSPO antibody (1:100; Abcam), rabbit anti-mouse CD11b antibody (1:100; Abcam), goat anti-mouse GFAP antibody (1:100; Abcam), rabbit anti-mouse macrophage antibody (1:100; Abcam), rat anti-mouse myeloperoxidase (MPO) antibody (1:100; Abcam), and rabbit anti-mouse CXCR4 antibody (1:100; Abcam). Secondary antibodies are Cy3-conjugated donkey anti-rabbit secondary antibody (1:200; Jackson ImmunoResearch Laboratories), Dylight 488-conjugated donkey anti-rabbit secondary antibody (1:200; Jackson ImmunoResearch Laboratories), and Cy3-conjugated donkey anti-goat secondary antibody (1:200; Jackson ImmunoResearch Laboratories). All brain tissue slices were mounted with medium containing 4',6-diamidino-2-phenylindole (DAPI) and then observed with an epifluorescence microscope (X81; Olympus).

Western Blot. Brain tissues were sonicated in T-per buffer (Thermo scientific) containing a protease inhibitor cocktail (Roche). After that, the protein suspension (40 µg) was separated on a 4 to 12% Bis-Tris gel using sodium dodecyl sulfate-polyacrylamide gel electrophoresis and transferred onto a polyvinylidene fluoride membrane. The membrane was blocked with blocking buffer (Thermo scientific) for 1 h at room temperature and incubated with specific primary antibody for TSPO (1:5000; Abcam) or SDF-1 (1:1000; Abcam)

overnight at 4 °C. After being washed three times with Tris-buffered saline containing 0.05% Tween 20, the membrane was subjected to a horseradish peroxidase-conjugated secondary antibody and detected by a SuperSignal West Pico Chemiluminescence Kit Detection System (Pierce).

Statistical Analysis. All data were expressed as means ± the standard deviation (means ± SD). Statistical analysis was performed with SPSS software (version 18.0, SPSS, Inc., Chicago, IL). One-way analysis of variance and a Student's *t* test were used for comparison of data between multiple groups and two groups, respectively. A *p* value of <0.05 was considered statistically significant.

RESULTS

$[^{18}\text{F}]$ DPA-714 PET Imaging of TSPO Expression. The successful establishment of the MCAO model was confirmed by T_2 -weighted MRI (Figure S1 of the Supporting Information). The high signal intensity that was observed in brain parenchyma was recognized as ischemic area and used as a reference to draw ROI on the corresponding PET images. A glucose uptake defect on the infarcted site by $[^{18}\text{F}]$ FDG PET can be seen on both days 1 and 3, followed by an obviously increased level of signal uptake on day 10. On day 16, the magnitude of the signal in the ischemic area dropped to a level similar to that in the sham (Figure S2 of the Supporting Information).

To evaluate TSPO overexpression in MCAO mice without any therapeutic intervention, the longitudinal PET using $[^{18}\text{F}]$ DPA-714 was performed on 0, 1, 3, 7, 10, and 16 days after surgery. As shown in Figure 1A, starting from day 3, an increased level of local uptake of $[^{18}\text{F}]$ DPA-714 in the ischemic area was observed, which peaked around day 10, and then the signal intensity dropped slowly until day 16. To further confirm

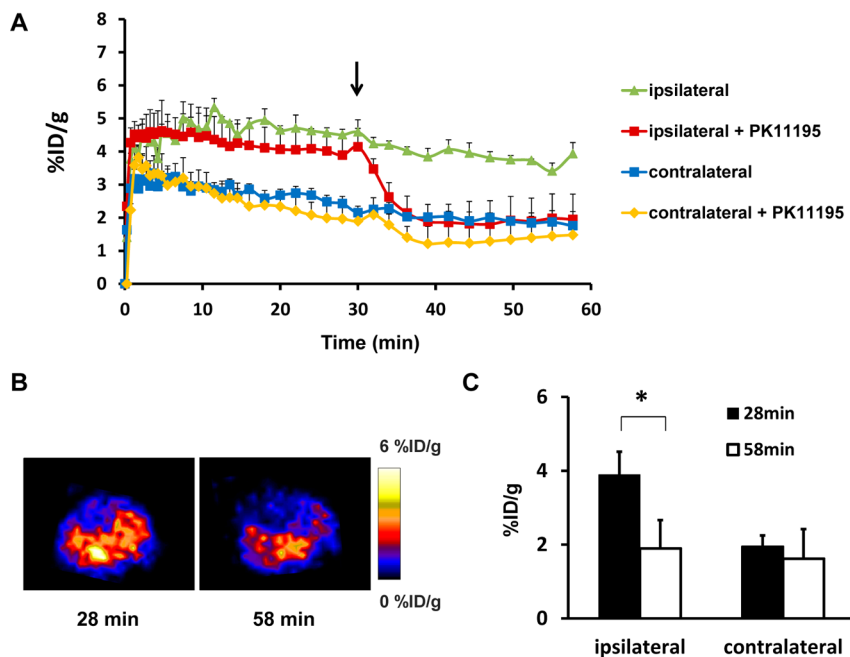


Figure 2. (A) $[^{18}\text{F}]$ DPA-714 displacement study using 5 mg of PK11195/kg 6 days after stroke. Time–activity curves of ROI placed on both the lesion and contralateral mirror area with or without PK11195 displacement, expressed as %ID/g of tissue. The arrow indicates the time point of PK11195 injection during the 1 h dynamic PET acquisition. (B) Representative coronal $[^{18}\text{F}]$ DPA-714 PET images of the brain acquired before and after PK11195 displacement. (C) $[^{18}\text{F}]$ DPA-714 uptake (%ID/g) of the lesion and healthy brain tissue before and after PK11195 injection (* $p < 0.05$).

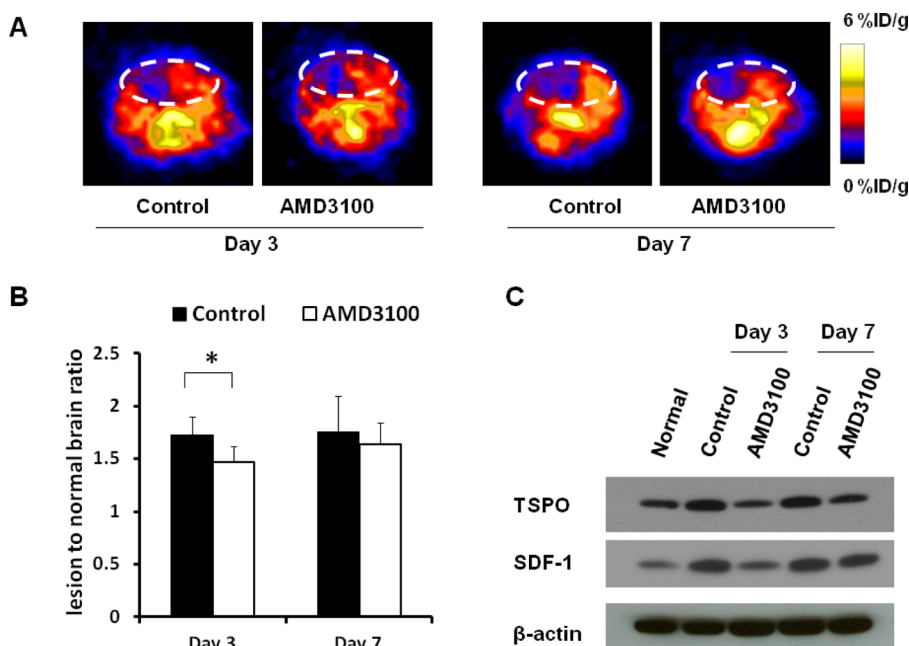


Figure 3. $[^{18}\text{F}]$ DPA-714 PET images of TSPO expression after AMD3100 treatment. (A) Representative coronal PET images of the AMD3100-treated group and normal saline-treated control group. (B) Quantification of the lesion-to-normal ratio showing a decreased signal intensity after AMD3100 treatment on days 3 and 7 (* $p < 0.05$). (C) Western blot assay showing the reduced TSPO protein level and SDF-1 expression in the AMD3100-treated group at targeted time points.

the location of the increased signal intensity on PET and facilitate the quantification of data, we performed T_2 -weighted MRI before PET imaging. As shown in Figure 1B, the fused images clearly showed a colocalization of the region of enhanced $[^{18}\text{F}]$ DPA-714 accumulation from PET and the ischemic area identified by MRI. Obviously, a high signal intensity can be observed on both the cortex and the basal area.

The lesion volume decreased gradually along with the pathologic progress, indicating the self-recovery and scar formation at late time points.

Quantitative results showed a significantly higher lesion-to-normal ratio in MCAO mice 1 day after surgery (1.37 ± 0.09) compared with the baseline level before surgery (1.09 ± 0.19) ($p < 0.05$). The ratio increased to 1.57 ± 0.17 , 1.67 ± 0.29 , and

2.04 ± 0.38 on days 3, 7, and 10, respectively. After that, the lesion-to-normal uptake ratio value dropped slightly to 1.80 ± 0.30 on day 16, which was still significantly higher than that in the control mice (Figure 1C).

To confirm the increased signal intensity in the ischemic area is a result of specific binding of [¹⁸F]DPA-714 to TSPO, a displacement study with unlabeled PK11195, a competitive TSPO ligand, was performed on three MCAO mice 6 days after surgery. As shown in Figure 2A, within a few minutes of injection of the tracer, the time–activity curve over the lesion area reached a plateau and showed a very slow downslope until 60 min. Upon injection of PK11195 at 30 min during the dynamic acquisition, the intensity of radioactivity dropped very rapidly. ROIs over the contralateral brain tissue generated a TAC with a much lower amplitude, and PK11195 injection showed a much less significant effect (Figure 2A). The signal intensity changes were also identified on PET images acquired before and after PK11195 displacement (Figure 2B). The amount of tracer uptake was significantly decreased after displacement at the lesion area [$3.89 \pm 0.63\text{ID/g}$ vs $1.95 \pm 0.77\text{ID/g}$ ($p < 0.05$)] but not in contralateral brain tissue [$1.90 \pm 0.30\text{ID/g}$ vs $1.62 \pm 0.80\text{ID/g}$ ($p > 0.05$)] (Figure 2C).

Change of TSPO Expression after AMD3100 Treatment. Because AMD3100 treatment interferes with the inflammatory process after ischemic brain injury, we performed *in vivo* PET imaging on both treated and control mice to follow the change in the level of TSPO. Three consecutive doses of treatment using AMD3100 did not fully block TSPO upregulation in the ischemic area. However, an apparently reduced [¹⁸F]DPA-714 signal intensity and signal volume can be seen in the AMD3100-treated group 3 days after surgery (Figure 3A), with a lesion-to-normal ratio of 1.47 ± 0.14 versus a value of 1.73 ± 0.17 ($p < 0.05$, compared with the saline only group). On day 7, the local level of tracer uptake is still somewhat lower in AMD3100-treated mice, but there was no significant difference between the two groups [1.64 ± 0.17 vs 1.75 ± 0.36 ($p > 0.05$)] (Figure 3B).

To confirm the PET findings, we collected the brain tissue and performed a Western blot study using TSPO specific antibodies. In normal brain tissues, there was a certain level of TSPO expression. Three days after surgery, the TSPO level increased dramatically and AMD3100 treatment reduced the TSPO protein level. Seven days after surgery, the TSPO level was still high and a decreased TSPO protein level in the AMD3100-treated group can be observed, but to a lesser extent (Figure 3C). To evaluate the SDF-1 expression after AMD3100 treatment, we performed a Western blot study in brain tissue with and without AMD3100 treatment on days 3 and 7. There was a low level of SDF-1 expression in healthy brain tissue and a significantly increased level of SDF-1 expression 3 and 7 days after stroke, and the SDF-1 level was decreased after AMD3100 treatment.

Immunohistological Staining of TSPO Expression. During neuroinflammation, TSPO upregulation was identified on several types of cells, including activated microglia, infiltrated neutrophils and macrophages, and astrocytes. Accordingly, we evaluated TSPO expression on brain slices harvested at different time points after MCAO, and CD11b and GFAP were chosen as markers for microglia and astrocytes, respectively. We found that the intensity of TSPO positive cells increased along with time with a peak appearing on day 10, which showed a time course similar to that for *in vivo* PET

results (Figure 4). Costaining with CD11b and GFAP revealed that microglia were the main cell type of TSPO positive cells at

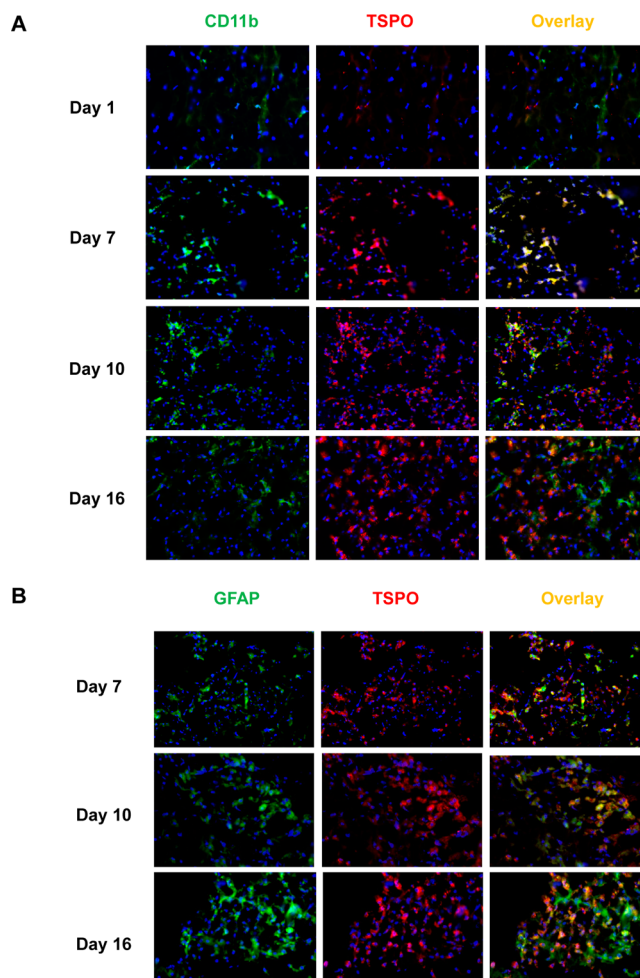


Figure 4. (A) Immunofluorescence staining of brain tissues harvested at different time points after MCAO surgery with anti-TSPO (red) and anti-CD11b (green) antibodies. (B) Immunofluorescence staining of brain slices at different time points after stroke with anti-TSPO (red) and anti-GFAP (green) antibodies. Nuclei are counterstained with DAPI (blue).

early time points. However, local astrocytes can also over-express TSPO at late stages of cerebral ischemia.

With AMD3100 treatment, the decreased intensity of TSPO positive cells in ischemic mouse brain was observed on day 3. On day 7, both treated and untreated groups presented a higher level of TSPO positive cells, but there was no significant difference between the two (Figure 5A). To further differentiate the source of TSPO protein, we performed immunofluorescence staining of macrophages and leukocytes. As shown in Figure 5B, AMD3100 treatment partially inhibited the accumulation of both macrophages and leukocytes in infarcted brain parenchyma on day 3, and the difference was diminished by day 7. The colocalized staining of macrophages and TSPO was performed on brain slices harvested on day 7. TSPO is positive for infiltrated macrophages after stroke but not limited to macrophages (Figure S4 of the Supporting Information).

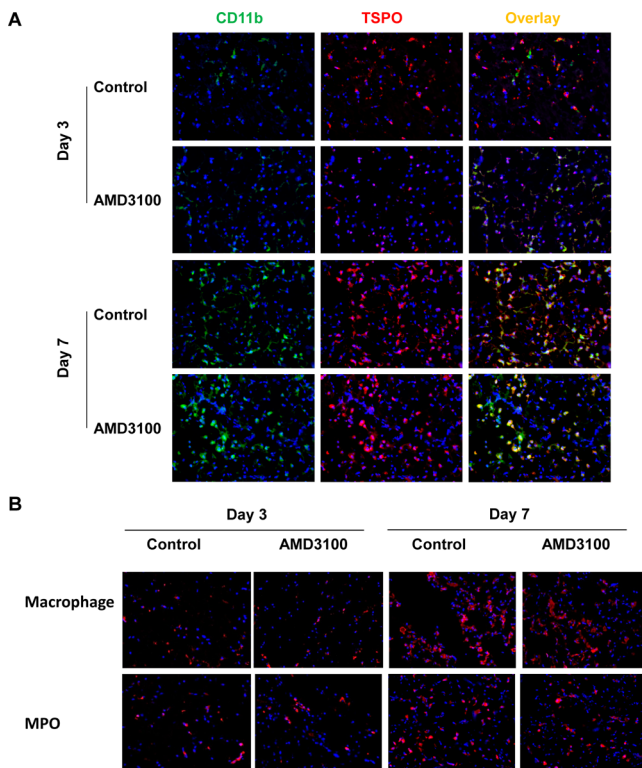


Figure 5. (A) Immunofluorescence staining of brain tissues from both the AMD3100-treated group and the control group with anti-TSPO (red) and anti-CD11b (green) antibodies. (B) Immunofluorescence staining of brain slices from both the AMD3100-treated group and the control group with anti-macrophage and anti-MPO antibodies. Nuclei are counterstained with DAPI (blue).

DISCUSSION

TSPO can be overexpressed on activated microglia and other cell types when the homogeneity in CNS is broken by internal or external factors. Hence, it has been intensively investigated as an imaging target for monitoring the inflammatory responses in different types of brain disease, including cerebral ischemia.^{18–20,27,34–38} Recently, several studies demonstrated the protective role of AMD3100 in experimental stroke.^{7,16} In particular, inhibition of the SDF-1/CXCR4 pathway during the acute stage after stroke promotes long-term recovery, mainly by depressing the extent of invasion of the ischemic territory by peripheral immune cells.¹⁶ Therefore, for the first time, to the best of our knowledge, we applied [¹⁸F]DPA-714 PET in monitoring the change in neuroinflammation induced by AMD3100 treatment in a mouse brain ischemia/reperfusion model.

Consistent with previous studies,²⁰ the time frame of the overexpression of TSPO can be dynamically monitored via longitudinal PET imaging using [¹⁸F]DPA-714 as the imaging tracer.³⁹ The specificity of [¹⁸F]DPA-714 to TSPO was confirmed by a displacement study with a mass amount of unlabeled PK11195. The local level of accumulation of [¹⁸F]DPA-714 increased significantly in ipsilateral ischemic side starting from day 3 after surgery and reached a peak on day 10. Then the signal intensity slightly dropped on day 16. Our study ended on day 16 after surgery instead of day 30 as in the previous report.²⁰ It is partially because mice are less tolerant to brain ischemia injury than rats. The high mortality rate of the model makes it difficult for long-term observation.

After ischemic injury in brain, the infarcted center and surrounding edema area have an increased amount of intracellular and extracellular water, leading to an obvious signal change on T₂-weighted MRI.⁴⁰ Coregistration of [¹⁸F]DPA-714 PET images with T₂-weighted MRI could provide anatomical reference to locate the PET signal. In most cases, we saw a relatively good overlay of the increased magnitude of the PET signal within the lesion site indicated by T₂-weighted MRI. However, at a late time point (day 16), the lesion area presented on MRI images was much smaller than the signal increased area on PET images. This may be due to the alleviation of edema at the late stage of the injury, and T₂-weighted MRI is not sufficiently sensitive to detect the lesion site.⁴¹

The small molecule SDF-1/CXCR4 inhibitor, AMD3100, has been shown to have a promising effect in attenuating ischemic injury in different animal models such as myocardial infarction, hindlimb ischemia, and stroke.^{7,16,42} The therapeutic effect of AMD3100 results from a reduction of the extent of infiltration of ischemic brain parenchyma by peripheral inflammatory cells. With [¹⁸F]DPA-714 PET, we observed a significant decrease in the magnitude of the signal after AMD3100 treatment on day 3, indicating that AMD3100 treatment downregulated the local TSPO protein level. This result was indeed confirmed by *ex vivo* Western blot and immunofluorescence staining against TSPO. However, the magnitude of the decrease in the signal intensity on PET images did not match perfectly with that from Western blots. In addition, the TSPO level decreased on day 7 with AMD3100 treatment on Western blot but was not detectable with PET. We speculate that this is partially due to the small size of the mouse brain and partial volume effect of PET imaging.⁴¹ It may also be related to the small dose of AMD3100 and the short drug delivery period.⁷ A decreased SDF-1 level was also observed after AMD3100 treatment, as shown by the Western blot study. The exact reason is unclear and needs to be investigated further.

Overexpression of TSPO in the ischemic brain area has been correlated with pathophysiological heterogeneity, such as microglia and astrocyte activation.^{43,44} Infiltrated peripheral immune cells, such as monocytes, leukocytes, and lymphocytes, also contribute to the overexpression of TSPO.²³ The signal of PET reflects the overall level of TSPO, which has no ability to differentiate the origination of the protein. Because AMD3100 can inhibit the SDF-1/CXCR4 pathway, resulting in decreased levels of migration of macrophages and/or leukocytes, it is highly possible that the decrease in the magnitude of the signal on PET images is caused by a decreased number of infiltrated peripheral lymphocytes. However, because of the nonspecificity of the cell maker of these cells,⁴⁵ we cannot exclude the contribution of activated microglia and astrocytes to the PET signal change. This is also supported by an incomplete colocalization of macrophages and TSPO.

Because of the complexity of the neuroinflammatory response after brain injury and intertwining of various cytokines and inflammatory cells, the dose and timing of therapeutic intervention would be very critical to the exertion of a beneficial effect and the prevention of any detrimental consequence in both acute and chronic phases. Although AMD3100 is promising in the treatment of experimental stroke, further investigation to optimize the therapy regimen is still needed for further clinical translation. We believe the accurate evaluation

of neuroinflammation with noninvasive imaging strategy would accelerate this process.

CONCLUSIONS

TSPO-targeted PET imaging using [¹⁸F]DPA-714 can be used to monitor the inflammatory response after stroke dynamically and noninvasively. Herein, [¹⁸F]DPA-714 can be a valuable probe for understanding the pathological process of neuroinflammation after stroke and provide a useful method for evaluating the therapeutic efficiency of the anti-inflammation treatment.

ASSOCIATED CONTENT

Supporting Information

Supplementary methods and figures. This material is available free of charge via the Internet at <http://pubs.acs.org>.

AUTHOR INFORMATION

Corresponding Authors

*Address: 9 Memorial Dr., 9/1W111, Bethesda, MD 20892. E-mail: niug@mail.nih.gov.

*Address: 87 Dingjiaqiao Rd., Nanjing, Jiangsu, China 210009. E-mail: gjteng@vip.sina.com.

*Address: 35A Convent Dr., GD937, Bethesda, MD 20892-3759. E-mail: shawn.chen@nih.gov.

Notes

The authors declare no competing financial interest.

ACKNOWLEDGMENTS

This work was supported by the National Basic Research Program of China (973 program, 2013CB733803, and 2013CB733802) and the Intramural Research Program (IRP) of the National Institute of Biomedical Imaging and Bioengineering, National Institutes of Health. We thank the Microscopy Imaging Core of the The Eunice Kennedy Shriver National Institute of Child Health and Human Development for their help with immunofluorescence staining.

REFERENCES

- (1) Go, A. S.; Mozaffarian, D.; Roger, V. L.; Benjamin, E. J.; Berry, J. D.; Borden, W. B.; Bravata, D. M.; Dai, S.; Ford, E. S.; Fox, C. S.; Franco, S.; Fullerton, H. J.; Gillespie, C.; Hailpern, S. M.; Heit, J. A.; Howard, V. J.; Huffman, M. D.; Kissela, B. M.; Kittner, S. J.; Lackland, D. T.; Lichtman, J. H.; Lisabeth, L. D.; Magid, D.; Marcus, G. M.; Marelli, A.; Matchar, D. B.; McGuire, D. K.; Mohler, E. R.; Moy, C. S.; Mussolini, M. E.; Nichol, G.; Paynter, N. P.; Schreiner, P. J.; Sorlie, P. D.; Stein, J.; Turan, T. N.; Virani, S. S.; Wong, N. D.; Woo, D.; Turner, M. B. Executive summary: Heart disease and stroke statistics—2013 update: A report from the American Heart Association. *Circulation* **2013**, *127* (1), 143–52.
- (2) Ceulemans, A. G.; Zgavc, T.; Kooijman, R.; Hachimi-Idrissi, S.; Sarre, S.; Michotte, Y. The dual role of the neuroinflammatory response after ischemic stroke: Modulatory effects of hypothermia. *J. Neuroinflammation* **2010**, *7*, 74.
- (3) Davalos, D.; Grutzendler, J.; Yang, G.; Kim, J. V.; Zuo, Y.; Jung, S.; Littman, D. R.; Dustin, M. L.; Gan, W. B. ATP mediates rapid microglial response to local brain injury *in vivo*. *Nat. Neurosci.* **2005**, *8* (6), 752–8.
- (4) Wieloch, T.; Nikolich, K. Mechanisms of neural plasticity following brain injury. *Curr. Opin. Neurobiol.* **2006**, *16* (3), 258–64.
- (5) Block, M. L.; Zecca, L.; Hong, J. S. Microglia-mediated neurotoxicity: Uncovering the molecular mechanisms. *Nat. Rev. Neurosci.* **2007**, *8* (1), 57–69.
- (6) Kim, H. J.; Chuang, D. M. HDAC inhibitors mitigate ischemia-induced oligodendrocyte damage: Potential roles of oligodendrogenesis, VEGF, and anti-inflammation. *Am. J. Transl. Res.* **2014**, *6* (3), 206–23.
- (7) Huang, J.; Li, Y.; Tang, Y.; Tang, G.; Yang, G. Y.; Wang, Y. CXCR4 antagonist AMD3100 protects blood-brain barrier integrity and reduces inflammatory response after focal ischemia in mice. *Stroke* **2013**, *44* (1), 190–7.
- (8) Zhu, Y.; Murakami, F. Chemokine CXCL12 and its receptors in the developing central nervous system: Emerging themes and future perspectives. *Dev. Neurobiol.* **2012**, *72* (10), 1349–62.
- (9) Schonemeier, B.; Schulz, S.; Hoell, V.; Stumm, R. Enhanced expression of the CXCL12/SDF-1 chemokine receptor CXCR7 after cerebral ischemia in the rat brain. *J. Neuroimmunol.* **2008**, *198* (1–2), 39–45.
- (10) Hill, W. D.; Hess, D. C.; Martin-Studdard, A.; Carothers, J. J.; Zheng, J.; Hale, D.; Maeda, M.; Fagan, S. C.; Carroll, J. E.; Conway, S. J. SDF-1 (CXCL12) is upregulated in the ischemic penumbra following stroke: Association with bone marrow cell homing to injury. *J. Neuropathol. Exp. Neurol.* **2004**, *63* (1), 84–96.
- (11) Cartier, L.; Hartley, O.; Dubois-Dauphin, M.; Krause, K. H. Chemokine receptors in the central nervous system: Role in brain inflammation and neurodegenerative diseases. *Brain Res. Brain Res. Rev.* **2005**, *48* (1), 16–42.
- (12) Jaerve, A.; Muller, H. W. Chemokines in CNS injury and repair. *Cell Tissue Res.* **2012**, *349* (1), 229–48.
- (13) White, F. A.; Bhangoo, S. K.; Miller, R. J. Chemokines: Integrators of pain and inflammation. *Nat. Rev. Drug Discovery* **2005**, *4* (10), 834–44.
- (14) Stumm, R. K.; Rummel, J.; Junker, V.; Culmsee, C.; Pfeiffer, M.; Kriegstein, J.; Holt, V.; Schulz, S. A dual role for the SDF-1/CXCR4 chemokine receptor system in adult brain: Isoform-selective regulation of SDF-1 expression modulates CXCR4-dependent neuronal plasticity and cerebral leukocyte recruitment after focal ischemia. *J. Neurosci.* **2002**, *22* (14), 5865–78.
- (15) Tanabe, S.; Heesen, M.; Yoshizawa, I.; Berman, M. A.; Luo, Y.; Bleul, C. C.; Springer, T. A.; Okuda, K.; Gerard, N.; Dorf, M. E. Functional expression of the CXC-chemokine receptor-4/fusin on mouse microglial cells and astrocytes. *J. Immunol.* **1997**, *159* (2), 905–11.
- (16) Ruscher, K.; Kuric, E.; Liu, Y.; Walter, H. L.; Issazadeh-Navikas, S.; Englund, E.; Wieloch, T. Inhibition of CXCL12 signaling attenuates the postischemic immune response and improves functional recovery after stroke. *J. Cereb. Blood Flow Metab.* **2013**, *33* (8), 1225–34.
- (17) Demerle-Pallardy, C.; Duverger, D.; Spinnewyn, B.; Pirotzky, E.; Braquet, P. Peripheral type benzodiazepine binding sites following transient forebrain ischemia in the rat: Effect of neuroprotective drugs. *Brain Res.* **1991**, *565* (2), 312–20.
- (18) Stephenson, D. T.; Schober, D. A.; Smalstig, E. B.; Mincy, R. E.; Gehlert, D. R.; Clemens, J. A. Peripheral benzodiazepine receptors are colocalized with activated microglia following transient global forebrain ischemia in the rat. *J. Neurosci.* **1995**, *15* (7, Part 2), S263–74.
- (19) Rojas, S.; Martin, A.; Arranz, M. J.; Pareto, D.; Purroy, J.; Verdaguer, E.; Llop, J.; Gomez, V.; Gispert, J. D.; Millan, O.; Chamorro, A.; Planas, A. M. Imaging brain inflammation with [¹¹C]PK11195 by PET and induction of the peripheral-type benzodiazepine receptor after transient focal ischemia in rats. *J. Cereb. Blood Flow Metab.* **2007**, *27* (12), 1975–86.
- (20) Martin, A.; Boisgard, R.; Theze, B.; Van Camp, N.; Kuhnast, B.; Damont, A.; Kassiou, M.; Dolle, F.; Tavitian, B. Evaluation of the PBR/TSPO radioligand [¹⁸F]DPA-714 in a rat model of focal cerebral ischemia. *J. Cereb. Blood Flow Metab.* **2010**, *30* (1), 230–41.
- (21) Yui, J.; Maeda, J.; Kumata, K.; Kawamura, K.; Yanamoto, K.; Hatori, A.; Yamasaki, T.; Nengaki, N.; Higuchi, M.; Zhang, M. R. ¹⁸F-FEAC and ¹⁸F-FEDAC: PET of the monkey brain and imaging of translocator protein (18 kDa) in the infarcted rat brain. *J. Nucl. Med.* **2010**, *51* (8), 1301–9.

- (22) Ruff, M. R.; Pert, C. B.; Weber, R. J.; Wahl, L. M.; Wahl, S. M.; Paul, S. M. Benzodiazepine receptor-mediated chemotaxis of human monocytes. *Science* **1985**, *229* (4719), 1281–3.
- (23) Canat, X.; Carayon, P.; Bouaboula, M.; Cahard, D.; Shire, D.; Roque, C.; Le Fur, G.; Casellas, P. Distribution profile and properties of peripheral-type benzodiazepine receptors on human hemopoietic cells. *Life Sci.* **1993**, *52* (1), 107–18.
- (24) Thiel, A.; Heiss, W. D. Imaging of microglia activation in stroke. *Stroke* **2011**, *42* (2), 507–12.
- (25) Chauveau, F.; Van Camp, N.; Dolle, F.; Kuhnast, B.; Hinnen, F.; Damont, A.; Boutin, H.; James, M.; Kassiou, M.; Tavitian, B. Comparative evaluation of the translocator protein radioligands ^{11}C -DPA-713, ^{18}F -DPA-714, and ^{11}C -PK11195 in a rat model of acute neuroinflammation. *J. Nucl. Med.* **2009**, *50* (3), 468–76.
- (26) Doorduin, J.; Klein, H. C.; Dierckx, R. A.; James, M.; Kassiou, M.; de Vries, E. F. $[^{11}\text{C}]$ -DPA-713 and $[^{18}\text{F}]$ -DPA-714 as new PET tracers for TSPO: A comparison with $[^{11}\text{C}]$ -(R)-PK11195 in a rat model of herpes encephalitis. *Molecular Imaging and Biology* **2009**, *11* (6), 386–98.
- (27) Boutin, H.; Prenant, C.; Maroy, R.; Galea, J.; Greenhalgh, A. D.; Smigova, A.; Cawthorne, C.; Julyan, P.; Wilkinson, S. M.; Banister, S. D.; Brown, G.; Herholz, K.; Kassiou, M.; Rothwell, N. J. $[^{18}\text{F}]$ DPA-714: Direct comparison with $[^{11}\text{C}]$ PK11195 in a model of cerebral ischemia in rats. *PLoS One* **2013**, *8* (2), e56441.
- (28) Arlicot, N.; Vercouillie, J.; Ribeiro, M. J.; Tauber, C.; Venel, Y.; Baulieu, J. L.; Maia, S.; Corcia, P.; Stabin, M. G.; Reynolds, A.; Kassiou, M.; Guilloteau, D. Initial evaluation in healthy humans of $[^{18}\text{F}]$ DPA-714, a potential PET biomarker for neuroinflammation. *Nucl. Med. Biol.* **2012**, *39* (4), 570–8.
- (29) Wang, Y.; Yue, X.; Kiesewetter, D. O.; Niu, G.; Teng, G.; Chen, X. PET imaging of neuroinflammation in a rat traumatic brain injury model with radiolabeled TSPO ligand DPA-714. *Eur. J. Nucl. Med. Mol. Imaging* **2014**, *41*, 1440–9.
- (30) Wu, C.; Yue, X.; Lang, L.; Kiesewetter, D. O.; Li, F.; Zhu, Z.; Niu, G.; Chen, X. Longitudinal PET imaging of muscular inflammation using ^{18}F -DPA-714 and ^{18}F -Alfatide II and differentiation with tumors. *Theranostics* **2014**, *4* (5), 546–55.
- (31) *Guide for the Care and Use of Laboratory Animals*; National Academy Press: Washington, DC, 2010.
- (32) Barone, F. C.; Knudsen, D. J.; Nelson, A. H.; Feuerstein, G. Z.; Willette, R. N. Mouse strain differences in susceptibility to cerebral ischemia are related to cerebral vascular anatomy. *J. Cereb. Blood Flow Metab.* **1993**, *13* (4), 683–92.
- (33) Wang, F.; Wang, Z.; Hida, N.; Kiesewetter, D. O.; Ma, Y.; Yang, K.; Rong, P.; Liang, J.; Tian, J.; Niu, G.; Chen, X. A cyclic HSV1-TK reporter for real-time PET imaging of apoptosis. *Proc. Natl. Acad. Sci. U.S.A.* **2014**, *111* (14), 5165–70.
- (34) Gerhard, A.; Neumaier, B.; Elitok, E.; Glatting, G.; Ries, V.; Tomczak, R.; Ludolph, A. C.; Reske, S. N. *In vivo* imaging of activated microglia using $[^{11}\text{C}]$ PK11195 and positron emission tomography in patients after ischemic stroke. *NeuroReport* **2000**, *11* (13), 2957–60.
- (35) Thiel, A.; Radlinska, B. A.; Paquette, C.; Sidel, M.; Soucy, J. P.; Schirrmacher, R.; Minuk, J. The temporal dynamics of poststroke neuroinflammation: A longitudinal diffusion tensor imaging-guided PET study with ^{11}C -PK11195 in acute subcortical stroke. *J. Nucl. Med.* **2010**, *51* (9), 1404–12.
- (36) Hossmann, K. A. Non-invasive imaging methods for the characterization of the pathophysiology of brain ischemia. *Acta Neurochirurgica. Supplement* **2003**, *86*, 21–7.
- (37) Lartey, F. M.; Ahn, G. O.; Ali, R.; Rosenblum, S.; Miao, Z.; Arksey, N.; Shen, B.; Colomer, M. V.; Rafat, M.; Liu, H.; Alejandre-Alcazar, M. A.; Chen, J. W.; Palmer, T.; Chin, F. T.; Guzman, R.; Loo, B. W., Jr.; Graves, E. The relationship between serial $[^{18}\text{F}]$ PBR06 PET imaging of microglial activation and motor function following stroke in mice. *Molecular Imaging and Biology* **2014**, *10*.1007/s11307-014-0745-0.
- (38) Lartey, F. M.; Ahn, G. O.; Shen, B.; Cord, K. T.; Smith, T.; Chua, J. Y.; Rosenblum, S.; Liu, H.; James, M. L.; Chernikova, S.; Lee, S. W.; Pisani, L. J.; Tirouvanziam, R.; Chen, J. W.; Palmer, T. D.; Chin, F. T.; Guzman, R.; Graves, E. E.; Loo, B. W., Jr. PET imaging of stroke-induced neuroinflammation in mice using $[^{18}\text{F}]$ PBR06. *Molecular Imaging and Biology* **2014**, *16* (1), 109–17.
- (39) James, M. L.; Fulton, R. R.; Vercoullie, J.; Henderson, D. J.; Garreau, L.; Chalon, S.; Dolle, F.; Costa, B.; Guilloteau, D.; Kassiou, M. DPA-714, a new translocator protein-specific ligand: Synthesis, radiofluorination, and pharmacologic characterization. *J. Nucl. Med.* **2008**, *49* (5), 814–22.
- (40) Wiart, M.; Davoust, N.; Pialat, J. B.; Desestret, V.; Moucharrafie, S.; Cho, T. H.; Mutin, M.; Langlois, J. B.; Beuf, O.; Honnorat, J.; Nighoghossian, N.; Berthezene, Y. MRI monitoring of neuroinflammation in mouse focal ischemia. *Stroke* **2007**, *38* (1), 131–7.
- (41) Soret, M.; Bacharach, S. L.; Buvat, I. Partial-volume effect in PET tumor imaging. *J. Nucl. Med.* **2007**, *48* (6), 932–45.
- (42) Jujo, K.; Ii, M.; Sekiguchi, H.; Klyachko, E.; Misener, S.; Tanaka, T.; Tongers, J.; Roncalli, J.; Renault, M. A.; Thorne, T.; Ito, A.; Clarke, T.; Kamide, C.; Tsurumi, Y.; Hagiwara, N.; Qin, G.; Asahi, M.; Losordo, D. W. CXC-chemokine receptor 4 antagonist AMD3100 promotes cardiac functional recovery after ischemia/reperfusion injury via endothelial nitric oxide synthase-dependent mechanism. *Circulation* **2013**, *127* (1), 63–73.
- (43) Capoccia, B. J.; Shepherd, R. M.; Link, D. C. G-CSF and AMD3100 mobilize monocytes into the blood that stimulate angiogenesis *in vivo* through a paracrine mechanism. *Blood* **2006**, *108* (7), 2438–45.
- (44) Rupprecht, R.; Papadopoulos, V.; Rammes, G.; Baghai, T. C.; Fan, J.; Akula, N.; Groyer, G.; Adams, D.; Schumacher, M. Translocator protein (18 kDa) (TSPO) as a therapeutic target for neurological and psychiatric disorders. *Nat. Rev. Drug Discovery* **2010**, *9* (12), 971–88.
- (45) Matsumoto, H.; Kumon, Y.; Watanabe, H.; Ohnishi, T.; Shudou, M.; Ii, C.; Takahashi, H.; Imai, Y.; Tanaka, J. Antibodies to CD11b, CD68, and lectin label neutrophils rather than microglia in traumatic and ischemic brain lesions. *J. Neurosci. Res.* **2007**, *85* (5), 994–1009.